System modeling and spatial sampling techniques for simplification of transition matrix in 3D Electronically Collimated SPECT

Anne C. Sauve[1], *Alfred O. Hero*[1], *W. Leslie Rogers*[2] *and Neal H. Clinthorne*[2]

January 15, 1997

Abstract

In this paper we will present numerical studies of the performance of a 3D Compton camera being developed at the University of Michigan. We present a physical model of the camera which exploits symmetries and an adapted spatial sampling pattern in the object domain. This model increases the sparsity of the transition matrix to reduce the very high storage and computation requirements. This model allows the decomposition of the transition matrix into several small blocks that are easy to store. Finally we discuss a real time algorithm which calculates entries of the transition matrix based on a Von Mises model for the conditional scatter angle distribution given the Compton energy measurement as well as a vector reformulation of the computation of the probabilities.

1 3D Compton scatter SPECT camera

Application of the Compton scatter aperture to imaging in nuclear medicine was first proposed in 1974 by Todd and Everett. This camera uses an innovative electronical cone-beam collimator based on the Compton scattering effect. Its requires a 3D image reconstruction. Singh [1] proposed in 1983 a linear image reconstruction for the Compton camera. This reconstruction is computationnally good but uses an inaccurate model of the system since it neglects the Poisson nature of the measurements. Leahy [2] implemented an MLE reconstruction from the transition matrix that takes into account the Poisson noise for a prototype system. This algorithm is computationnally demanding since a 3D image of moderate size (128^3 pixels) requires already a very big matrix T (resp 128^6).

Background

The aperture consists of a position sensitive solid state detector ($\det_1$) with a high energy resolution. This detector is paired with a second position sensitive detector, $\det_2$, which can be a scintillation camera with lower energy resolution.

[1]A. Sauve (corresponding author : asauve@engin.umich.edu) and A. Hero are with the Dept. of Electrical Engineering and Computer Science, The University of Michigan, Ann Arbor, MI 48109-2122.

[2]L. Rogers and N. Clinthorne are with the Dept. of Nuclear Medicine, The University of Michigan, Ann Arbor, MI 48109-0552.

Figure 1: Illustration of the Compton scatter collimator

The γ rays from the point source, X, that reach $\det_1$ are Compton scattered by the solid state detector, $\det_1$ (Fig. 2). Those scattered photons are then detected by the second detector in coincidence with the events in $\det_1$. The energy deposited in $\det_1$ increases as a function of the scattering angle θ according to Compton scattering statistics.

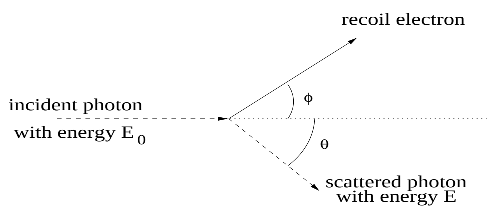

Figure 2: The Compton scatter effect

Since the vector describing the scattered photon is known from the two position signals, the direction of the original photon can be computed within a conical ambiguity.

Although mechanical collimation is simple and relatively inexpensive to implement, it has the fundamental drawback that it has a poor sensitivity. Even in the case of the pinhole collimator and without considering attenuation and scatter effects, only about 10^{-4} of the emitted photons are detected based on geometric factors alone.

Efforts have been made to develop electronical collimators. Those collimators, since they utilize as many emitted photons as possible from all directions, improve the solid angle of detection and therefore provide an improved detection efficiency and sensitivity over mechanical collimators.

For the Compton scatter collimator, each resolution element of det_1 can be thought of as a "pinhole" whose response function at each energy interval is an ellipse on the surface of det_2. Sensitivity gains derive from the fact that, unlike the case for a real pinhole, a resolution element in det_2 is sensitive to primary γ rays incident from many angles. Further, since the position of the scatter event in det_1 is known, the number and density of these resolution elements may be increased without introducing any ambiguity involving the particular "pinhole" the photon passed through. This means that the sensitivity increases in approximate proportion to the solid angle subtended by det_1.

It has been shown that we can detect 60 times more photons with such a collimator than with a comparable mechanical cone-beam collimator, [3]. Moreover, electronical collimation provides multiple views simultaneously.

One of the open questions is whether it will be possible to attain equivalent or better resolution than with pinhole collimators using fast algorithms based on sparse matrix computations and sparse systems modeling.

2 Analytical model using Von Mises density

As with many statistical imaging systems, the camera is entirely defined by its transition matrix T. We developed a program that analytically computes T. This eliminates the need for Monte Carlo simulations for determining the transition matrix. Then, we developed a simplified model for the camera so that T will be easy to manipulate, i.e. sparse and well conditioned. It is important to simplify the structure of T as much as possible to implement computationally tractable 3D reconstructions and to optimize the system through CR bound computations.

Analytical computation of T

The elements of the transition matrix T of the camera are the joint probabilities $P(d_2, E, d_1|x)$, often called transition probabilities, where:

$$\begin{cases} \mathrm{d}_2 \text{ : det}_2 \text{ cell where scattered photon is recorded,} \\ \mathrm{d}_1 \text{ : det}_1 \text{ cell where incident photon is scattered,} \\ \mathrm{E} \text{ : detected Compton energy,} \\ \mathrm{x} \text{ : a source point.} \end{cases}$$

A cell d_2 is completely defined by the two scattering angles θ and ϕ (Fig. 3).

We assume the azimuthal angle ϕ to be uniformly distributed

$$P(\phi|\theta, d_1, x) = \frac{1}{2\pi}.$$

From the Compton relation the energy ϵ of the scattered photon and the scatter angle θ are related by [4]:

$$\epsilon = \frac{\epsilon_0}{1 + \alpha(1 - \cos\theta)}.$$

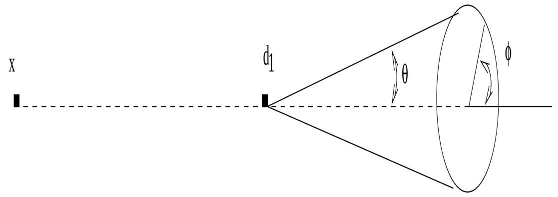

Figure 3: definition of the angles

The conditional distribution of ϵ given emitter position x and detector cell d_1 is given by the **Klein-Nishina distribution** [4] :

$$P(\epsilon|d_1, x) = \frac{.572}{\epsilon_0}\left[1 + \left(2 - \frac{\epsilon_0}{\epsilon}\right)^2 + \left(1 - \frac{\epsilon_0}{\epsilon}\right)^2 \frac{\epsilon}{\epsilon_0}\right].$$

In the classical approach, the conditional distribution of the detected energy E ($E = \epsilon + n$) given θ, d_1 and x is assumed to be Gaussian [1]. However, this is a non-physical model even for variance of moderate magnitude since it assigns non-zero probability to negative values of E. Under the Gaussian assumption, the joint probability of an incident event received in detector cell d_2 and energy bin E given d_1 and x can be computed by:

$$P(d_2, E|d_1, x) = \frac{P_{1C}}{2\pi} \iint_{\Omega} P(E|\theta, \phi, d_1, x) \, P(\theta|d_1, x) d\theta d\phi.$$

Here P_{1C} is the probability of a single Compton scatter in det_1 (here we assume negligible photo-electric absorption) and Ω is the set of angles (θ, ϕ) which define rays passing through position x, d_1 to the surface of the cell d_2.

The Von Mises model described below is an alternative which ensures that negative energy measurements are assigned probability zero. First, since it is more convenient to measure the energy E instead of the angle θ we express $P(\theta|d_1, x)$ as a function of $P(E|d_1, x)$. Using the Compton and the Klein-Nishina relations, we can make the following **change of variable** :

$$P(E|d_1, x) = \left|\frac{d\theta}{dE}\right| P(\theta|d_1, x) \mid_{\theta = \theta(E)}.$$

The Von Mises model specifies the conditional distribution of the scattering angle θ given E, d_1 and x as a **Von Mises** distribution [5] with centrality parameter $\arccos(2 - \frac{E_0}{E})$ and width parameter β:

$$P(\theta|E, d_1, x) = \frac{\exp\left[\beta \cos\left(\theta - \arccos\left(2 - \frac{E_0}{E}\right)\right)\right]}{2\pi I_0(\beta)},$$

where $I_0(\beta)$ is the modified Bessel function of the first kind and β is a shape parameter which we estimate from Monte Carlo simulations. The Von Mises model is physically appropriate for the angle distribution because it is 2π periodic.

Using the Von Mises conditional density for θ we get:

$$P(d_2,E|d_1,x) = \frac{P_{1C}}{2\pi} \iint_{\Omega} P(\theta|E,d_1,x)P(E|d_1,x)d\phi d\theta.$$

Under the assumption that d_2 cell surface area is small with respect to the spread $\frac{1}{\beta}$ of the Von Mises density, this integral relation can be approximated.

$$P(d_2,E|d_1,x) = \frac{P_{1C}}{2\pi}\, P(E|d_1,x)\, \frac{\Delta S}{2\pi I_0(\beta)\|\overrightarrow{d_1 d_2}\|^2}$$
$$\exp\left[\beta\left((2-\frac{E_0}{E})\sqrt{1-\frac{\|P_{\perp}^{\overrightarrow{d_1 x}}(\overrightarrow{d_1 d_2})\|}{\|\overrightarrow{d_1 d_2}\|^2}} + \frac{\|P_{\perp}^{\overrightarrow{d_1 x}}(\overrightarrow{d_1 d_2})\|}{\|\overrightarrow{d_1 d_2}\|^2}\sqrt{1-(2-\frac{E_0}{E})^2}\right)\right]$$

where the projection into plane with normal $\overrightarrow{d_1 x}$ is denoted by the operator: $P_{\perp}^{\overrightarrow{d_1 x}} = I - \frac{(\overrightarrow{d_1 x})(\overrightarrow{d_1 x})^T}{\|\overrightarrow{d_1 x}\|^2}$, and ΔS is the $\det_2$ pixel area.

The above expression is rich in vector operations and is therefore suitable for fast on line computation. Note that when $\overrightarrow{d_1 d_2}$ has constant length and the pixel areas ΔS are constant, the p.d.f. $P(d_2,E|d_1,x)$ has symmetries which can be exploited to reduce computation. This occurs when the detector $\det_2$ is an hemisphere centered at d_1. Let $P(d_1|x)$ be the probability that a γ-ray emitted at x, intercepts the detector surface d_1 (computed from the solid angle subtended by the cell d_1 from the source point x). This probability when combined with the above relation gives the required elements of the transition matrix from:

$$P(d_2,E,d_1|x) = P(d_2,E|d_1,x)\,P(d_1|x),$$

indexed over d_2, E and d_1.

Symmetry exploitation

We first assume that $\det_2$ is an hemisphere and that $\det_1$ is a unique cell at the center of $\det_2$. As we will show, this

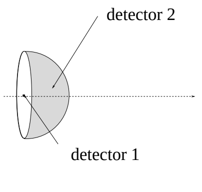

Figure 4: Camera Model

greatly reduces the storage and computation requirements due to resulting symmetries in the transition matrix.

The measurement equation can be written as:

$$\mathbf{y} = T\,Q\,\lambda + N,$$

where $\mathbf{y}$ is a vector containing the measured coincidence events, T is the system matrix, Q is a cartesian to hemispherical bilinear interpolation matrix [6], λ is the image

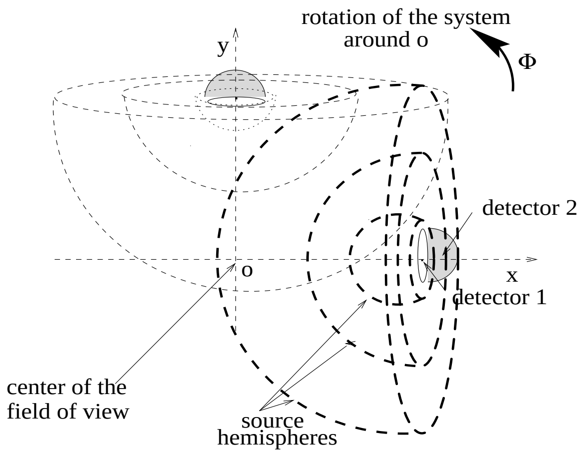

Figure 5: Hemispherical source sampling and Rotation of the detectors 1 and 2 around the field of view

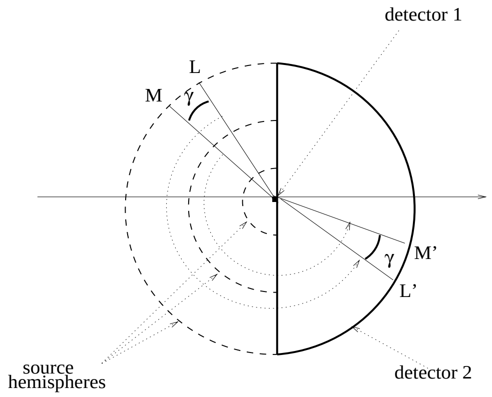

Figure 6: Source emissions leading to event trajectories (LL') and (MM'), respectively, have identical transition probabilities.

to be reconstructed (ie the source intensity) in cartesian coordinates, and N accounts for system mismodeling errors and counting statistics of the Poisson events.

T can be arranged as a the concatenation of the transition matrices obtained for the p different Compton energies E_i, and Q is the concatenation of the interpolation matrices for the n different rotations of the system:

$$T = \begin{bmatrix} T_{E_1} \\ \vdots \\ T_{E_p} \end{bmatrix}, \quad Q = \begin{bmatrix} Q^{\Phi_1} \\ \vdots \\ Q^{\Phi_n} \end{bmatrix}.$$

We can write $T_{E_j} = [H_{E_j} R]$ where:
$$\begin{cases} H_{E_j} = \big(\big(\,P(d_2,E_j|d_1,x)\,\big)\big)_{\mathbf{d_2},\mathbf{x}}, \\ R = [\rho_1 I_k \ldots \rho_L I_k]. \end{cases}$$

- k is the number of source pixels on one hemisphere and l is the number of hemispheres intersecting the field of view.
- H_{E_j} contains the transition probabilities for the energy E_j when d_2 varies over $\det_2$ and x varies over a single hemisphere of the source.

- ρ_i is the solid angle subtended by d_1 from the hemisphere i.

Finally, the transition matrix can be written in the compact form:

$$T = \begin{bmatrix} H_{E_1} R \otimes I_k \\ \vdots \\ H_{E_p} R \otimes I_k \end{bmatrix}.$$

Because we uniformly sample over a hemispherical grid in object space, H_{E_j} does not depend on the particular hemisphere. Moreover, H_{E_j} depends on relative angles only and is therefore approximately circulant and diagonalizable via 2D FFT methods. R also is very sparse. This structure for T will significantly simplify the computationally demanding 3D reconstruction algorithms. Moreover, we do not have to store the very large T matrix but only the H_{E_j} and the L scalars ρ_i leading to reduction of storage requirements by several orders of magnitude.

Annulus sinogram obtained for this camera model

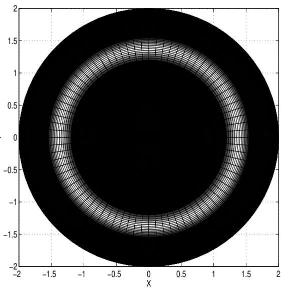

Figure 7: Planar projection of the sinogram obtained on det_2 from a $511kev$ photon coming initially from a point on the camera symmetry axis and that Compton scattered from det_1 with $E = 400Kev$ (for $\beta = 700$ and 6400 cells in det_2).

3 CR Bound for 3D Reconstruction Tasks

The uniform CR bound [7] provides a lower bound on the variance of any estimator with bias gradient length bounded by the user specified parameter $\delta > 0$. It is a useful tool for establishing fundamental performance limitations of tomographic systems [8]. With $\hat{g}$ an estimator of a smooth function $g = g(\lambda)$ of the 3D intensity λ the bound is of the form

$$\mathrm{var}(\hat{g}) \geq [e_1 + d]^T F_\lambda^+ [e_1 + d]$$

where e_1, d_1 are vectors related to g, δ and F_λ are described in [7], A^+ denotes pseudoinverse of a matrix A, and F_λ is the Fisher information matrix

$$F_\lambda = Q^T T^T \Sigma^{-1} T Q.$$

Here $\Sigma = \mathrm{diag}(TQ\lambda)$ is a diagonal matrix constructed from the vector of mean system responses to a source of intensity λ. The matrix F_λ is symmetric of dimension $m^3 \times m^3$ where m^3 is the number of pixels in the (presumed cubic) imaging volume. Even for relatively small problems it is not practical to attempt to invert F_λ directly. By exploiting the sparseness and symmetry of the transition matrix T we develop fast recursive equation solvers to calculate the CR bound for 3D reconstruction tasks such as uptake and contrast estimation in a region of interest. The bound is used obtain estimator-independent comparisons between different camera configurations, e.g. spatial sampling and interpolation schemes, Compton scatter energy resolution, and number of camera rotation angles. These results will be presented in the full paper.

References

[1] M. Singh and D. Doria, "An electronically collimated gamma camera for single photon emission computed tomography. part II: Image reconstruction and preliminary experimental measurements," *Transactions on Medical Physics*, vol. 10, no. 4, pp. 428–435, 1983.

[2] T. Hebert, R. Leahy, and M. Singh, "Maximum likelihood reconstruction for a prototype electronically collimated single photon emission system," in *Proc. SPIE Medical Imaging*, vol. 767, pp. 77–83, 1987.

[3] M. Singh, "An electronically collimated gamma camera for single photon emission computed tomography. part I: Theoretical considerations and design criteria," *Transactions on Medical Physics*, vol. 10, pp. 421–427, July/August 1983.

[4] G. F. Knoll, *Radiation Detection and Measurement.* Wiley, 1979.

[5] N. I. Fisher, T. Lewis, and B. J. J. Embleton, *Statistical Analysis of Spherical Data.* Cambridge University Press, 1987.

[6] R. N. Bracewell, *Two-Dimensional Imaging.* Prentice Hall, 1995.

[7] A. O. Hero, J. A. Fessler, and M. Usman, "Exploring estimator bias-variance tradeoffs using the uniform CR bound," *IEEE Transactions on Signal Processing*, vol. 44, no. 8, pp. 2026–2041, 1996.

[8] N. H. Clinthorne, C. yi Ng, C. ho Hua, J. E. Gormley, J. W. Leblanc, S. J. Wilderman, and W. L. Rogers, "Theoretical performance comparison of a compton-scatter aperture and parallel-hole collimator." To appear in the Conference Record of the 1996 IEEE Nuclear Science Symposium, 1996.